# Quantitative Analysis of Gas Circuit Breaker Physics Through Direct Comparison of 3-D Simulations to Experiment

Nils P. Basse, *Member, IEEE*, Margarita Martinez Abrahamsson, Martin Seeger, *Senior Member, IEEE*, and Torsten Votteler

***Abstract*—Understanding the dynamic processes governing gas circuit breaker physics is crucial in order to continue to improve short-circuit current interruption performance. In this paper, we study a single arc discharge both using measurements and 3-D computational fluid dynamics simulations. The primary quantity analyzed is the pressure in the heating volume created by radiative ablation of the Polytetrafluoroethylene nozzles surrounding the arc. We use cross-correlation functions to investigate the behavior of pressure waves in the $SF_6$ gas, especially those induced at flow reversal where the gas flow between the arc zone and heating volume changes direction.**

***Index Terms*—Computational fluid dynamics (CFD), cross-correlation function, gas circuit breaker, pressure waves.**

## I. Introduction

The ARC zone of high-voltage self-blast gas circuit breakers is challenging to diagnose directly due to the combination of temperatures in the 30 000 K range and densities of order $10^{25}$ m$^{-3}$. Instead, proxy measurements are made, typically in the heating volume of the breakers. In this paper, we compare pressure measurements of the $SF_6$ gas from two sensors to 3-D computational fluid dynamics (CFD) simulations. The simulated pressure evolution is analyzed at the same position as the actual sensors are placed, so in that sense the CFD simulations can be thought of as a synthetic diagnostic [1]. The overarching purpose of this quantitative comparison of CFD simulations with measurements is to improve our understanding of the physics of current interruption in gas circuit breakers. Further, questions will be generated in the case where agreement is poor between simulation and experiment. This in turn guides us as to what should be: 1) modified in the simulation and/or 2) additionally measured to answer the questions posed and thereby improve our knowledge of the physical processes.

Manuscript received August 24, 2007; revised March 14, 2008. Current version published November 14, 2008.

N. P. Basse, M. Seeger, and T. Votteler are with Corporate Research, ABB Switzerland Ltd., 5405 Baden-Dättwil, Switzerland (e-mail: nils.basse@ch.abb.com; martin.seeger@ch.abb.com; torsten.votteler@ch.abb.com).

M. M. Abrahamsson was with Corporate Research, ABB Switzerland Ltd., 5405 Baden-Dättwil, Switzerland (e-mail: margarita.abrahamsson@gmail.com).

Digital Object Identifier 10.1109/TPS.2008.2004235

This paper is organized as follows. In Section II, we describe the arc discharge treated; we introduce the 3-D CFD simulation in Section III. The comparison between measured and simulated heating volume pressures is to be found in Section IV. Finally, we present our conclusions in Section V.

## II. Discharge Description

The basic layout of a gas circuit breaker is shown in Fig. 1; only the upper half of the breaker is shown. Initially, the plug contact is physically touching the finger contact (or tulip). When high current is to be interrupted, the contacts separate and an arc forms between them. The sequence of events leading to current interruption is the following.

1) Radiation from the arc causes ablation of the polytetrafluoroethylene (PTFE) nozzle, leading to flow from the high pressure arc zone to the heating volume; this is known as backheating. In the case of high current, the arc is said to be ablation controlled at this time [3].
2) Pressure increases in the heating volume and begins to decrease in the arc zone as current zero (CZ) is approached and ablation is reduced. At the time when the heating volume pressure equals the arc zone pressure flow reversal takes place.
3) Flow is thereafter directed from the heating volume to the arc zone and the arc is axially blown [4].
4) The arc is extinguished at CZ.

Arc current and voltage for the discharge analyzed is shown in Fig. 2. Current is limited to two half-waves by a vacuum circuit breaker. CZ is after the second half-wave at zero seconds on the time axis. The rise of the arc voltage defines the time of contact separation, leading to an arcing time of 15 ms. The current peaks are strongly asymmetric due to the setup of the test circuit.

Just before the second current half-wave reaches CZ, the breaker is stressed by the application of a transient recovery voltage (TRV) as shown in Fig. 3. The oscillations in the TRV after the initial peak are due to the inductive component of the circuit. The high voltage circuit used to generate the TRV is separate from the high current circuit creating the arc; the combined circuit is known as a Weil-Dobke circuit [5].

The measured heating volume pressure using sensors hv1 and hv2 is shown in Fig. 4. The qualitative behavior is the same for the two measurements, with a maximum pressure of about

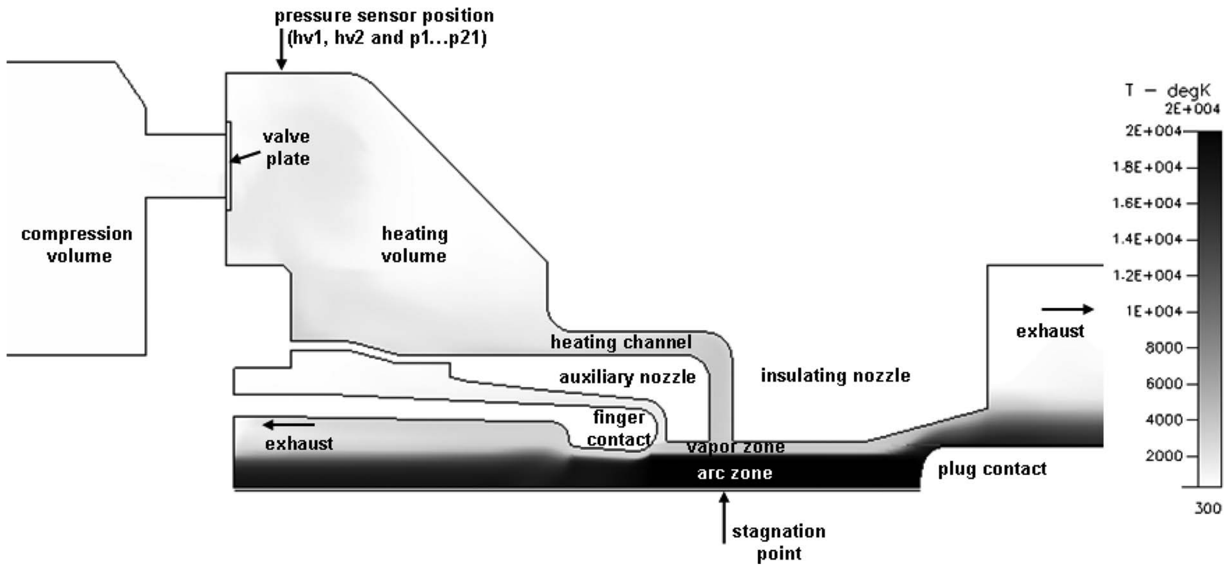


Fig. 1. Gas circuit breaker sketch adapted from [2]. The greyscale is the simulated temperature at the peak of the second current half-wave.

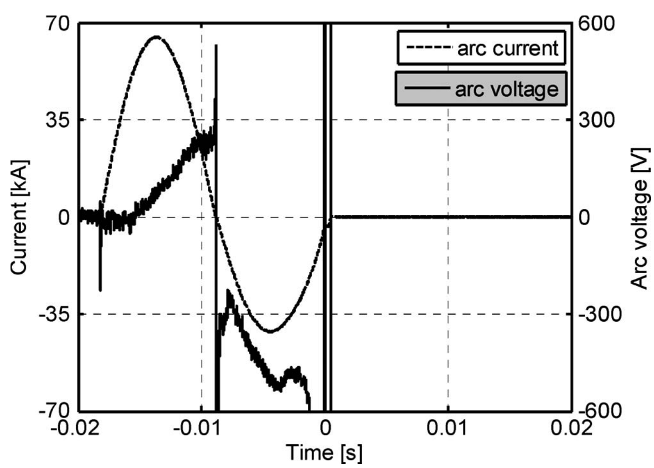


Fig. 2. Arc current (dashed) and voltage (solid).

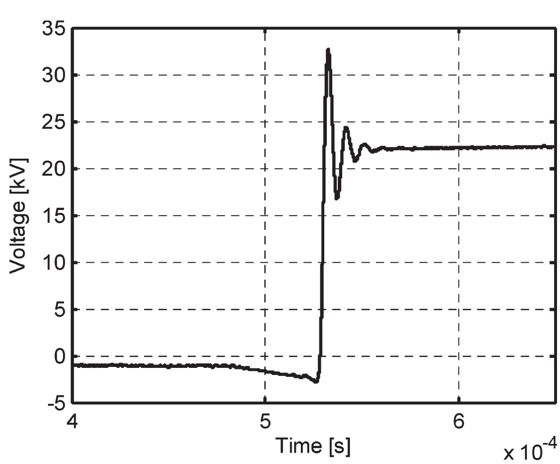


Fig. 3. Transient recovery voltage generated by the high-voltage part of the circuit. The maximum $dv/dt$ is about 11 kV/$\mu$s.

25 bar a few milliseconds after the peak of the second current half-wave. Pronounced oscillations are observed both during the high current phase and after CZ.

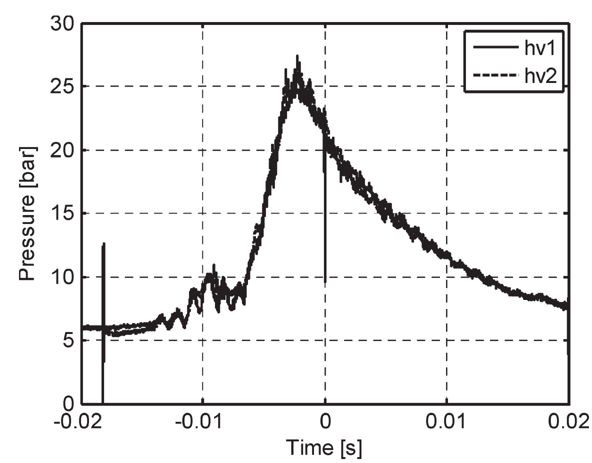


Fig. 4. Measured heating volume pressure using sensors hv1 (solid) and hv2 (dashed). Pressure is shown in bar.

## III. CFD Simulation

### A. Implementation

*1) Equation System Solved and the Arc Model:* The physical model used in the simulation is a simplified integral model called the two-zone model [6], where the arc zone is divided into two isothermal zones: 1) a conducting arc zone and 2) a non conducting PTFE vapor layer surrounding the arc. The two zones are indicated in Fig. 1.

The two-zone model offers a well understood and computationally efficient method of simulating the high-current arc in an $SF_6$ gas circuit breaker. One major advantage of the model is that it does not require the solution of the equations for the electromagnetic field and radiation transport. Therefore, it can be implemented in any flow solver. There is essentially a one-way coupling between the flow and the arc, i.e., the flow is driven by Ohmic heating from the arc, but the properties of the arc do not depend on the flow in any consequential way [7].

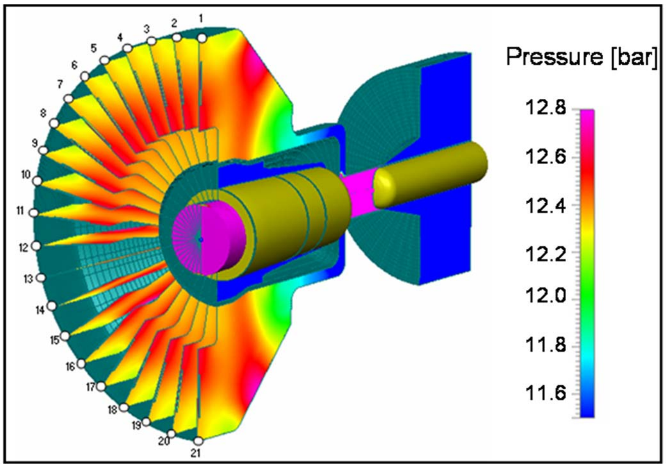


Fig. 5. Simulated pressure with the 21 pressure monitor points marked. Monitor points 1 and 21 are 180° apart.

The implementation herein is characterized by the following features.

- The simulation uses the two-zone model for ablation controlled arcs and the Lowke approximation [8] for axially blown arcs. This makes it possible to simulate the whole arcing process.
- The full geometry of the breaker is simulated, complete with the motion of the plug, the piston in the puffer, and the moving valve plates.
- The geometry of the breaker and the two zones (arc and vapor) are all assumed to be completely axisymmetric. There are no asymmetric parts in the geometry used for this investigation.
- Simulations can be run with or without turbulence. Neglecting turbulence is a simple way of speeding up the simulations without losing too much accuracy, especially since the two-zone model already makes a large number of simplifying assumptions. Turbulence is not included in the simulation described in this paper.
- The model only considers PTFE ablation in the nozzle. The rate of mass ablated is given by the two-zone model and is inserted as a source of mass only to the cells next to the wall of the nozzle where the ablation occurs. The PTFE mass ablation is distributed uniformly over the length of the ablation walls.
- The interruption performance of a gas circuit breaker depends strongly on the properties of the enclosed gas. The CFD solver uses real gas data, accessible during the computation.

*2) Calculation Software:* A commercial CFD solver is used to solve the differential equations on a specified grid. It solves the Navier–Stokes equations numerically in cylindrically symmetric problems, either 2-D or 3-D.

For 3-D, which we use in this paper, one employs an appropriate "wedge" of the model. We apply 40 cells to cover a wedge angle of 180°, see Fig. 5 for an illustration.

It is important to point out that ***the flow calculated is fully 3-D***. In contrast, the circuit breaker geometry and the arc and vapor zones are treated as being 2-D. The resulting flow varies azimuthally. This is mainly due to the nonlinear nature of the Navier–Stokes equations. A way to visualize this is to consider a von Kármán vortex street, e.g., vortices generated by flow around a cylinder [9]. Here, a symmetric flow toward the cylinder will generate vortices in the wake of the cylinder, thus breaking the symmetry.

TABLE I
CELL SIZES FOR CFD SIMULATION

| Volume | Cell size [mm] |
|---|---|
| Arc | 0.3-1 |
| Channels | 1-4 |
| Heating volume | 2-6 |
| Compression volume | 5-8 |
| Diffusers | 3-6 |

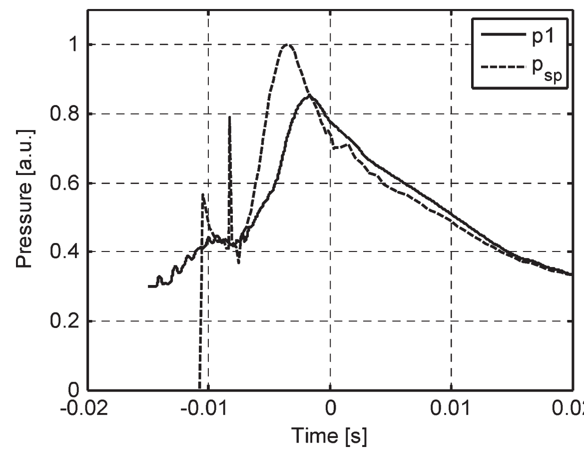


Fig. 6. Heating volume pressure at monitor point 1 (p1, solid) and at the stagnation point of the arc zone ($p_{sp}$, dashed).

The CFD solver allows grid deformation for transient simulations with moving parts.

*3) Grid and Time Step:* The cell sizes in Table I are typical values used to mesh circuit breaker geometries when applying the two-zone model. The total number of cells simulated is about 250 000.

Results are almost identical if the number of cells is reduced by a factor of two.

Note that the arc volume needs high grid refinement. The cell sizes in the other volumes could increase gradually around the baseline values provided.

The optimal time step is 10–20 $\mu$s.

### B. Results

At the time displayed in Fig. 5, a pressure wave in the heating volume can clearly be seen originating where the heating channel is connected to the heating volume. We use simulated pressure at monitor points 1 and 21 and compare to the two measurements, also positioned 180° apart.

The simulated pressure in the arc zone at the stagnation point (sp) and at one of the monitor points in the heating volume (p1) is shown in Fig. 6. The stagnation point is situated where the heating channel joins the arc zone, see Fig. 1. Therefore, the pressure at this position is zero until the plug has moved past the stagnation point. After this occurs, the stagnation point

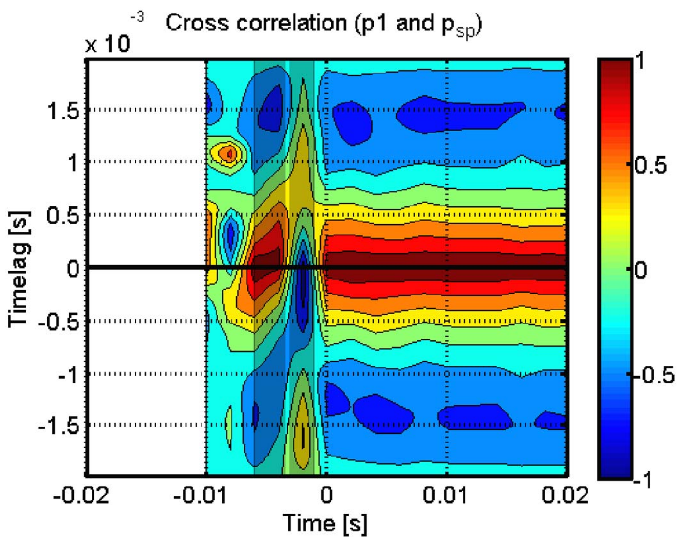


Fig. 7. Cross-correlation function between simulated heating volume and arc zone pressure (shown in Fig. 6). Red (blue) is due to correlated (anti-correlated) structures. The two semi transparent grey rectangles indicate the features discussed in the main text.

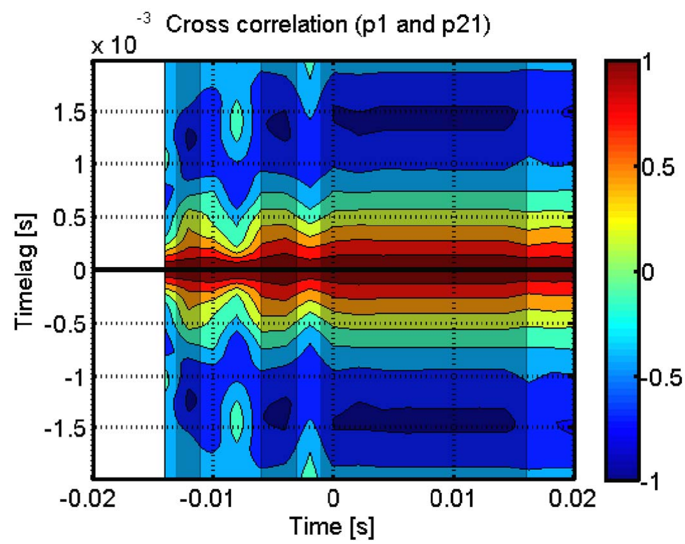


Fig. 8. Cross-correlation function between simulated heating volume pressure in monitor points 1 and 21. The three semi transparent grey rectangles indicate the features discussed in the main text.

pressure jumps up to the arc zone pressure. Flow reversal takes place 2 ms before CZ. The spike in the stagnation point pressure at −8 ms is due to a convergence problem in the simulation.

To quantify the transient behavior associated with flow reversal, we calculate the cross correlation function (also known as the normalized cross covariance function) [10] between the heating volume and arc zone pressures, see Fig. 7. A negative timelag means that the event first takes place in the heating volume, thereafter in the arc zone.

Two features can be observed.

1) At −6 ms a correlated (red), oscillating structure is seen. The peak is at zero timelag, so the event is occurring at the same time for both positions. The period can be estimated to 2.8 ms from the anti correlated (blue), symmetric troughs at +/−1.4 ms.
2) At −2 ms an anti correlated, oscillating structure is seen, The peak is at −0.2 ms and the period is roughly as before, namely 2.8 ms.

The transition between these two features coincides with the flow reversal time and the second feature can be interpreted as a simultaneous reduction of the heating volume pressure and small increase of the arc zone pressure (anti correlation).

The physical processes from flow reversal onwards can be understood as follows [11].

1) Hot (about 5000 K) gas from the heating channel begins to flow to the arc zone because of the pressure reduction there.
2) Outflow of colder (< 2000 K) gas from the heating volume starts, highly subsonic at first.
3) The pressure increases slightly in the arc zone, but remains below the heating volume pressure because of energy dissipation in the heating channel.
4) Flow from the heating volume to the arc zone stops and the arc zone pressure decreases.
5) When the arc zone pressure is below the heating channel pressure by a certain amount, cold gas from the heating channel flows to the arc zone and stops the pressure decay there.
6) A smaller increase of the arc zone pressure occurs and the cycle starts again.
7) Since these cycles are in cold gas at this late time, oscillation amplitudes are low and heavily damped.

## IV. Comparison Between Measurement and Simulation

The cross correlation between the simulated pressure at monitor points 1 and 21 is shown in Fig. 8.

Three pressure oscillations can be identified:

1) a feature at −12 ms with a period of 2.4 ms;
2) a feature at −5 ms with a period of 2.6 ms;
3) a feature after CZ with a period of 2.8 ms.

The first two features are associated with the two current half-waves and the resulting pressure buildup. The final oscillations after CZ are in cold gas.

The cross correlation in Fig. 8 can be directly compared to the cross correlation between the measured heating volume pressures, also positioned 180° apart, see Fig. 9.

Features 2 and 3 from Fig. 8 are also observed in the measurements with the same period.

One can combine information on the oscillation periods found above with the circuit breaker geometry and simulated pressure using four steps.

1) The distance between the heating volume pressure sensor location and the stagnation point along with the time delay between them is used to construct the average velocity, $v_{\mathrm{average}}$, between the two points.
2) The simulated ratio between the arc zone and heating volume pressures can be used to construct the Mach

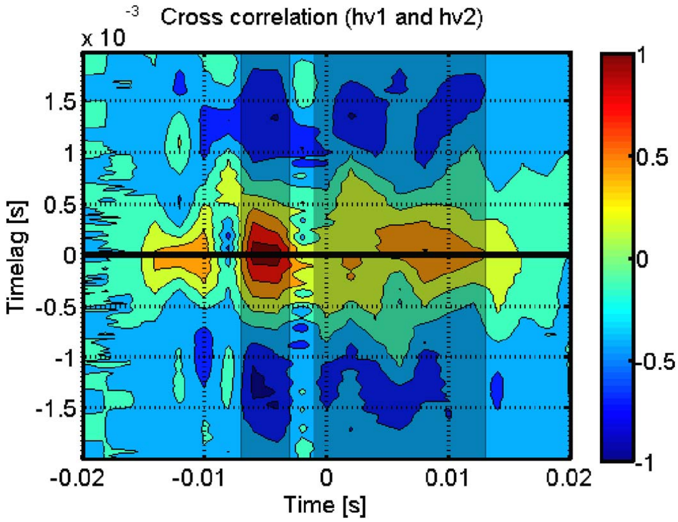


Fig. 9. Cross-correlation function between measured heating volume pressure 180° apart (shown in Fig. 4). The two semi transparent grey rectangles indicate the features discussed in the main text.

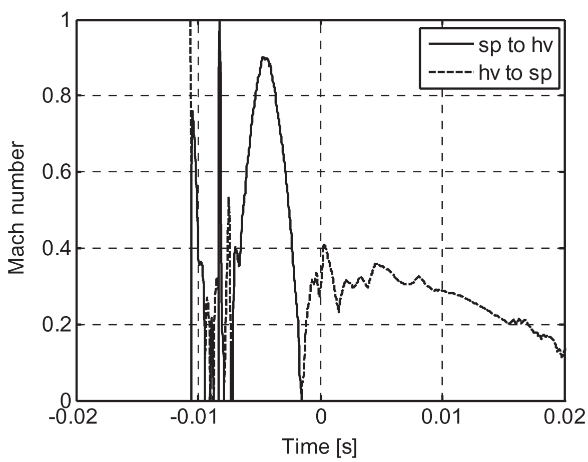


Fig. 10. Mach number found from the CFD simulation and (1). The solid line is flow from the arc zone to the heating volume and the dashed line is flow from the heating volume to the arc zone.

number $(Ma)$ between the locations according to

$$\left(\frac{p_{\mathrm{position1}}}{p_{\mathrm{position2}}}\right)^{\frac{\gamma-1}{\gamma}} = 1 + \frac{\gamma - 1}{2} \times Ma^2 \tag{1}$$

3) where $\gamma$ is the adiabatic coefficient, see Fig. 10 [12]. Note that (1) is only valid for an adiabatic flow. The equation is applicable in our situation, since we use the Mach number to calculate an average temperature. We take $\gamma$ to be 1.1, which is the value for 1500 K. The Mach number is quite insensitive to the chosen $\gamma$.
4) The sound speed is found from

$$v_{\mathrm{sound}} = \frac{v_{\mathrm{average}}}{Ma}. \tag{2}$$

5) The calculated sound speed yields the average temperature. In Fig. 11 we show the sound speed versus temperature for pressures of 1 and 25 bar. The sound speed is independent of pressure up to 1500 K and increases with the square root of temperature.

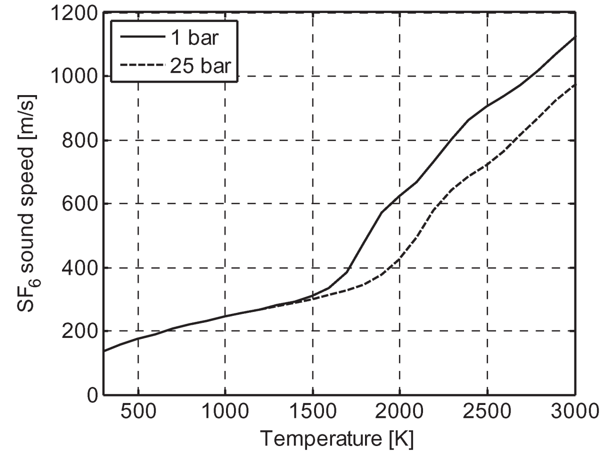


Fig. 11. Sound speed versus temperature for 1 bar (solid) and 25 bar (dashed).

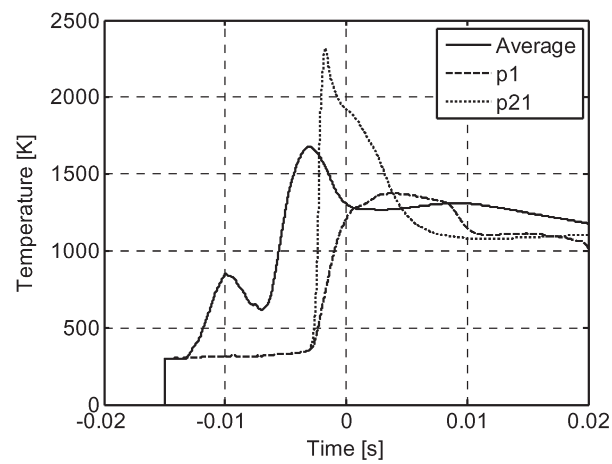


Fig. 12. Simulated temperatures: Average in heating volume (solid) and at pressure sensor location 1 (dashed) and 21 (dotted).

Using this technique we calculate the average temperature for feature 3, see Figs. 8 and 9. The average speed is of the order 100 m/s and we derive the following temperature: $T_{\mathrm{feature3}} = 1600$ K. The average simulated heating volume temperature for the feature is about 1200 K, see Fig. 12. We conclude that the simulated temperature is about 25% below the estimate using the measured oscillation period.

Our simple estimate of an average temperature from a combination of simulation and measurements is a basic consistency check and shows that discrepancies exist.

## V. Conclusion

In this paper, we have compared a 3-D CFD simulation of a high voltage gas circuit breaker to measurements.

Our focus was an analysis of pressure; the simulated and measured pressures were post processed using cross correlation functions. The results showed similar oscillatory features in both data sets. The oscillations are due to the transient pressure buildups during high current arcing. The resulting pressure differences between the arc zone and the heating volume lead to the periodic behavior.

We estimated the average gas temperature in the circuit breaker by combining the measured and simulated pressure.

Temperature measurements would be necessary to check the predictions.

Future modifications to improve the simulation include (i) a more exact treatment of the arc radiation and (ii) the addition of a turbulence model. The choice of turbulence model should ideally be based on turbulence measurements.

## REFERENCES


[1] M. Greenwald, "Beyond benchmarking—How experiments and simulations can work together in plasma physics," *Comput. Phys. Commun.*, vol. 164, no. 1–3, pp. 1–8, Dec. 2004.

[2] C. M. Franck and M. Seeger, "Application of high current and current zero simulations of high-voltage circuit breakers," *Contrib. Plasma Phys.*, vol. 46, no. 10, pp. 787–797, Nov. 2006.

[3] M. Seeger, L. Niemeyer, T. Christen, M. Schwinne, and R. Dommerque, "An integral arc model for ablation controlled arcs based on CFD simulations," *J. Phys. D, Appl. Phys.*, vol. 39, no. 10, pp. 2180–2191, May 2006.

[4] W. Hermann, U. Kogelschatz, K. Ragaller, and E. Schade, "Investigation of a cylindrical, axially blown, high-pressure arc," *J. Phys. D, Appl. Phys.*, vol. 7, no. 4, pp. 607–619, Mar. 1974.

[5] R. D. Garzon, *High Voltage Circuit Breakers*, 2nd ed. New York: Marcel Dekker, 2002, ch. 9.

[6] L. Niemeyer, "Evaporation dominated high current arcs in narrow channels," *IEEE Trans. Power App. Syst.*, vol. PAS-97, no. 3, pp. 950–958, May 1978.

[7] M. Claessens, "Simulation von Gasströmungen in SF6-Selbstblasschaltern bei Kurzschlussabschaltung," Ph.D. dissertation, RWTH-Aachen, Aachen, Germany, 1997.

[8] J. J. Lowke and H. C. Ludwig, "A simple model for high-current arcs stabilized by forced convection," *J. Appl. Phys.*, vol. 46, no. 8, pp. 3352–3360, Aug. 1975.

[9] U. Frisch, *Turbulence: The legacy of A.N. Kolmogorov*. Cambridge, U.K.: Cambridge Univ. Press, 1995, ch. 1.

[10] J. S. Bendat and A. G. Piersol, *Random Data*, 3rd ed. New York: Wiley, 2000.

[11] M. Seeger and A. Dahlquist, *CFD Study on Pressure Oscillations in High Voltage Circuit Breakers*, 2003.

[12] R. D. Blevins, *Applied Fluid Dynamics Handbook*. New York: Van Nostrand, 1984, pp. 126–127.



**Nils P. Basse** (M'06) received the B.Sc., M.Sc., and Ph.D. degrees from the Niels Bohr Institute, University of Copenhagen, Copenhagen, Denmark, in 1996, 1998, and 2002, respectively.

He is a Scientist with ABB Switzerland Ltd., Corporate Research, Baden-Dättwil, Switzerland. He was a Postdoctoral Associate at the Plasma Science and Fusion Center, Massachusetts Institute of Technology, Cambridge, from 2002 to 2005. His present research interests include plasmas in medium- and high-voltage circuit breakers.



**Margarita Martinez Abrahamsson** was born in Bogotá, Colombia, on August 29, 1980. She received the Industrial Engineering degree from the Pontificia Universidad Javeriana, Bogotá, in 2003.

From 2002 to 2008, she worked for ABB Sweden and ABB Switzerland in different positions. She was with Corporate Research, ABB Switzerland Ltd., Baden-Dättwil, for three years.


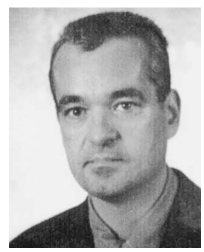


**Martin Seeger** (M'04–SM'07) was born in Giessen, Germany, on January 19, 1961. He received the M.S. and Ph.D. degrees in physics from the University of Heidelberg, Heidelberg, Germany, in 1987 and 1990, respectively.

Since 1993, he has been with ABB Switzerland Ltd. in different positions. Since 2000, he has been with Corporate Research, Baden-Dättwil.



**Torsten Votteler** was born in Bellikon, Switzerland, in 1971. He received the Dipl.El.Ing. degree from the Fachhochschule Aargau, Aargau, Switzerland, in 2000.

Since 2001, he has been with Corporate Research, ABB Switzerland Ltd., Baden-Dättwil, Switzerland.